metals

MDPI

Article

Influence of Heat Input on Microstructure and Mechanical Properties of Gas Tungsten Arc Welded HSLA S500MC Steel Joints

Kianoosh Kornokar [1], Fardin Nematzadeh [1,*], Hossein Mostaan [1], Amirhossein Sadeghian [2], Mahmoud Moradi [2,3,*], David G. Waugh [2] and Mahdi Bodaghi [4,*]

[1] Department of Materials and Metallurgical Engineering, Faculty of Engineering, Arak University, Arak 38156-88349, Iran; kornokarkianosh@gmail.com (K.K.); h-mostaan@araku.ac.ir (H.M.)
[2] Faculty of Engineering, Environment and Computing, School of Mechanical, Aerospace and Automotive Engineering, Coventry University, Gulson Road, Coventry CV1 2JH, UK; sadeghiana@uni.coventry.ac.uk (A.S.); ac4963@coventry.ac.uk (D.G.W.)
[3] Department of Mechanical Engineering, Faculty of Engineering, Malayer University, Malayer 65719-95863, Iran
[4] Department of Engineering, School of Science and Technology, Nottingham Trent University, Nottingham NG11 8NS, UK
* Correspondence: f-nematzadeh@araku.ac.ir (F.N.); ad6683@coventry.ac.uk (M.M.); mahdi.bodaghi@ntu.ac.uk (M.B.)

Abstract: High-strength low alloy (HSLA) S500MC steel is widely used for chassis components, structural parts, and pressure vessels. In this study, the effects of heat input during automatic gas tungsten arc welding (GTAW) on microstructure and mechanical properties of thermomechanically controlled processed (TMP) S500MC steel were investigated. A butt joint configuration was used, and welding was performed in autogenous mode. Six different levels of heat input namely 1.764 kJ/mm, 1.995 kJ/mm, 2.035 kJ/mm, 2.132 kJ/mm, 2.229 kJ/mm, and 2.33 kJ/mm were considered. Microstructural investigations revealed a different microstructure than base metal in the fusion zone (FZ) of all welded joints which was most likely due to a lath martensitic microstructure surrounded by retained austenite. With increased heat input, the amount of retained austenite and the size of packets increased. In the heat-affected zone (HAZ), two distinct regions of coarse grain (CG-HAZ) and fine grain (FG-HAZ) were observed. Due to the presence of carbides in the HAZ, mostly a martensitic microstructure with smaller packets, compared to FZ, was formed. By increasing the heat input and through the dissolution of carbides, the dimension of packets increased. Due to microstructural changes and grain growth, in both the FZ and the HAZ, the mechanical properties produced by TMP were lost in these regions. However, failure occurred in the base metal of all samples with a maximum tensile strength of 690 MPa. Thus, tensile strength in the weld zone and HAZ were higher than the base metal even for the highest heat input indicating the formation of a good joint between S500MC plates with GTAW, regardless of heat input.

Keywords: gas tungsten arc welding (GTAW); heat input; S500MC steel; microstructure; mechanical properties

Citation: Kornokar, K.; Nematzadeh, F.; Mostaan, H.; Sadeghian, A.; Moradi, M.; Waugh, D.G.; Bodaghi, M. Influence of Heat Input on Microstructure and Mechanical Properties of Gas Tungsten Arc Welded HSLA S500MC Steel Joints. *Metals* **2022**, *12*, 565. https://doi.org/10.3390/met12040565

Academic Editors: Francisco J. G. Silva and António Bastos Pereira

Received: 27 February 2022
Accepted: 25 March 2022
Published: 27 March 2022

1. Introduction

Gas tungsten arc welding (GTAW), also known as tungsten inert gas (TIG) is a conventional arc welding technique in which a non-consumable tungsten electrode creates an arc on the workpiece [1]. GTAW has several advantages over other arc welding methods such as good metallurgical and mechanical properties of welds between almost all metals including dissimilar ones [2]. Moreover, GTAW normally creates spatter-free joints with minimum distortion and a narrow heat-affected zone (HAZ) [3]. However, it is well-known

that the quality of welds produced with fusion welding processes is highly dependent on selecting suitable process parameters [4].

S500MC is a grade of high-strength low alloy (HSLA) steels that are normally developed by thermomechanical processing (TMP) [5]. Small quantities of carbide and nitride-forming elements such as Ti, Nb, and V are present in the chemical composition of HSLA steels. These elements are responsible for the high strength as a result of grain refinement and precipitation hardening [6,7]. HSLA steels are used for welded components in various applications such as construction, transport, and off-shore structures due to their superior combination of strength, toughness, and formability [8,9]. Although S500MC steel possesses good weldability owing to relatively low carbon levels, the effect of heat input and cooling rate during welding can easily alter the microstructure of the fusion zone (FZ) and the HAZ through the formation of hard and brittle phases such as a martensitic structure, thereby diminishing the mechanical properties [10]. Furthermore, the susceptibility of S500MC steel to cold cracking in the fusion zone has been reported in the literature [11].

Several studies have been conducted on the weldability of HSLA steels and the effects of process parameters on the weld geometry and phase transformations in the FZ and the HAZ during fusion welding [12–15]. Musa et al. investigated the effect of GTAW parameters on the microstructure and microhardness of the HAZ in L450 HSLA steel. It was concluded that welding parameters had a massive effect on the hardness profile and microstructural features of welds [16]. The increase of welding heat input resulted in an increase in the width of HAZ and the growth of prior austenite grains. A relationship between weld microstructure and mechanical properties in HSLA steels was established by Oyyaravelu et al. They observed martensitic structure in the weld zone due to very high cooling rates [17]. Miletić et al. studied the properties of HSLA steel welded joints. They reported a decrease in impact toughness of S690QL steel due to the increase in welding heat input [18]. The impact of GTAW parameters on the weld bead profile of 15CDV6 HSLA steel was studied by Skariya et al. using an optimization approach to maximize the depth of penetration while minimizing the HAZ [19]. In a similar study, a Taguchi Optimization technique was used by Pamnani in GTAW of DMR 249 A HSLA steel to optimize the process parameters to achieve the highest depth of penetration [20]. The relationship between fatigue and fracture ductile-Brittle transition in S500 welds was studied by Salabba et al. [21]. They reported a constant reduction in fatigue crack propagation rate with decreasing test temperature even below the ductile-brittle transition temperature.

GTAW is a cost-effective process and can easily be automated which makes it important to optimize the process parameters in the GTAW of S500MC. Despite the advances, the influence of heat input on the phase transformations during the GTAW of S500MC HSLA steel has not been fully understood yet. The tensile strength of a weld is highly dependent on microstructure which is determined by microstructural changes induced by welding conditions. In the present study, the effect of welding heat input on microstructure, and tensile strength of gas tungsten arc welded joints was investigated. Six levels of heat input from low to high were compared in terms of their effect on the FZ and the HAZ microstructure and the mechanical properties of joints.

2. Materials and Methods

For this study, HSLA S500MC steel plates were mechanically cut into 60 mm × 30 mm × 1.5 mm pieces. The chemical composition of S500MC steel based on quantometer analysis is listed in Table 1. The equivalent carbon content (CE) was calculated in accordance with Equation (1) [22] as 0.39 indicating good weldability. The mechanical properties of S500MC based on standard EN 10,025 are presented in Table 2.

$$CE_{IIW} = C + \frac{Mn}{6} + \frac{Cu + Ni}{15} + \frac{Cr + Mo + V}{5} \quad (1)$$

Table 1. Chemical composition of S500MC (wt.%).

Element	Fe	C	Si	Mn	Ni	Cu	P	Cr	Mo	S	Al	V	Ti
Composition	Bal.	0.11	0.14	1.64	0.0075	0.016	0.01	0.03	0.021	0.002	0.05	0.004	0.004

Table 2. Mechanical properties of S500MC.

Elongation (%)	Tensile Strength (MPa)	Yield Strength (MPa)
≥14	550–700	≥500

Before welding, surface oxides were removed by grinding, and then acetone was used to clean any residue or grease on the joint surfaces. A square groove with a root opening of 0.5 mm was used for welding. Experiments were carried out with an automatic GTAW system on an adjustable welding table. The tungsten electrode contained 2% thorium and the diameter was 3.2 mm. The welding torch angle was placed at 60° to the horizontal surface. Welding was performed with direct current electrode negative (DCEN) for lower spatter and a more stable arc. No filler metal was used for welding. During the welding, argon gas with a purity of 99.98% was used as the shielding gas. The gas flow rate was 10 L/min. To reduce welding-induced distortion, samples were fixed during the experiments using a fixture. Welding was carried out in one pass and with a butt-welding configuration. Welding parameters used in this study are presented in Table 3. To investigate the influence of heat input on microstructure and tensile strength of joints, various welding currents and speeds were selected to adjust the heat input for each experiment. Voltage and arc length was kept at a constant level. Heat input, one of the most important parameters in GTAW, was calculated for each set of welding parameters using Equation (2) [23].

$$H = \frac{V * I * 60}{1000 * S} \quad (2)$$

where H is heat input (kJ/mm), V is voltage (V), I is current (A), and S is welding speed (mm/min). The calculated heat input value for each experiment based on Equation (2) is also presented in Table 3. Schematics of the GTAW process and actual welding of S500MC steel in butt configuration are presented in Figure 1a,b, respectively.

Table 3. Welding parameters used in experiments.

Experiment No.	Current (A)	Voltage (V)	Arc Length (mm)	Welding Speed (mm/min)	Heat Input (kJ/mm)
1	105	21	3	75	1.764
2	95	21	3	60	1.995
3	105	21	3	65	2.035
4	110	21	3	65	2.132
5	115	21	3	65	2.229
6	120	21	3	65	2.33

To study the microstructure, specimens were cut in the middle of the weld line transverse to the welding direction and then were subjected to grinding using SiC abrasive papers up to 2500 grade. Next, samples were polished to a 1 µm finish, followed by etching in 2% Nital solution for 10 s. Meiji IM-7200 inverted metallurgical microscope (Meiji Techno, San Jose, CA, USA) was used for microstructural investigations. Tensile tests were carried out on standard tensile samples to study the mechanical properties of joints. Tensile test specimens were extracted using electrical discharge machining (EDM) according to standard ASTM-E8. Tensile tests were conducted at room temperature and with an overhead speed of 2 mm/min. A VEGA TESCAN-XMU scanning electron microscope

(SEM, TESCAN, Brno, The Czech Republic) was used for examining the fractured surface of joints.

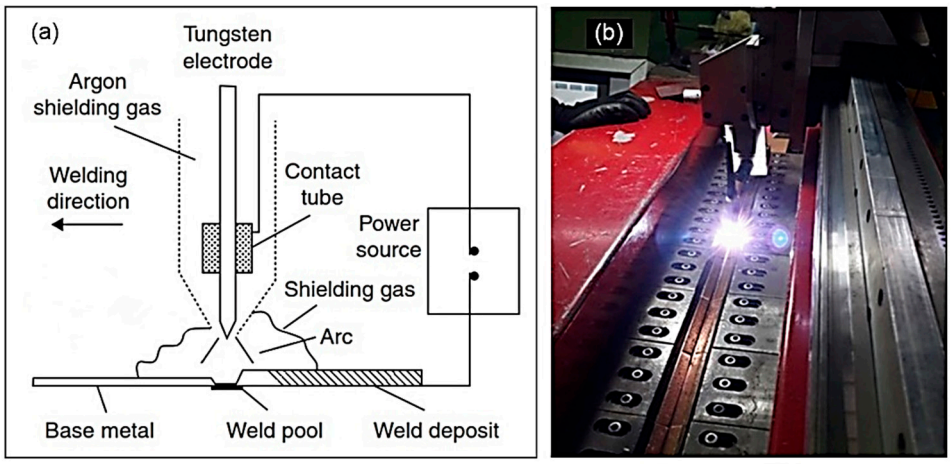

Figure 1. (**a**) Schematics of GTAW process, (**b**) GTAW of S500MC steel in butt configuration.

3. Results and Discussion

3.1. Microstructure

Figure 2 shows the microstructure of base metal before welding. As can be seen, the base metal microstructure consisted of ferrite (light areas) and pearlite (dark areas) with small grain size as a result of prior thermomechanical treatment. The microstructure of the base metal was in a normalized state.

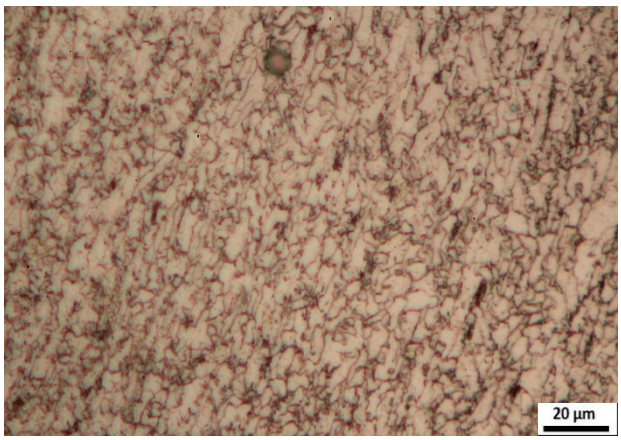

Figure 2. S500MC HSLA steel microstructure consisting of ferrite (light areas) and pearlite (dark areas).

The optical micrograph of sample No. 5 is illustrated in Figure 3. The welded joint can be divided into weld metal (WM), coarse grain (CG-HAZ), fine grain (FG-HAZ), and base metal. Columnar grain growth towards the center of weld and mostly in the opposite direction of heat flow can be observed at the interface of the weld zone. By increasing the welding power or decreasing the welding speed the heat input increased. In all weld samples, with heat inputs ranging from 1.764 kJ/mm to 2.33 kJ/mm, complete penetration was observed with the width of fusion zone, CG-HAZ, and FG-HAZ all increasing with the increase in heat input. The fusion zone width increased from 3.7 mm in sample No. 1 to 5.5 mm in sample No. 6. The increase in weld width, due to the increase in heat input, during fusion welding S700MC steel has been reported by Tomkow et al. [24]. Weld geometry is very important in GTAW and can determine the mechanical properties. Complete penetration was observed in welded samples. Suitable weld depth and width indicated proper welding parameters. Furthermore, no macro defects such as cracks or pores were observed. Figure 4 illustrates the effect of heat input on the fusion zone microstructure in

welded samples. Fusion zone microstructure was most likely composed of lath martensitic microstructure surrounded by retained austenite due to the high hardenability of S500MC. By increasing the heat input the amount of retained austenite was increased due to an increase in peak temperature. Moreover, higher heat input increased the size of martensite packets due to more cooling time. Other researchers have also discussed the influence of heat input on retained austenite and the size of martensitic structure [25,26]. This is due to the fact that during the welding process micro-alloyed carbides were dissolved removing the barrier for grain growth, resulting in coarse grains in the fusion zone compared to the base metal. Four factors generally determine the final microstructure of low carbon low alloy steels: cooling time, alloying elements, size of initial austenite, and the amount of oxygen [27]. Due to the autogenous nature of welding in this investigation, the amount of oxygen was identical in all samples. The amount of alloying elements was also similar. It was observed that increasing the heat input caused the dissolution of precipitates and increased the size of martensite packets. More cooling time promoted the formation of coarser martensite and increased the amount of retained austenite. Thus, in this study cooling time and initial austenite grain size, which were affected by heat input, determined the final microstructure of welds.

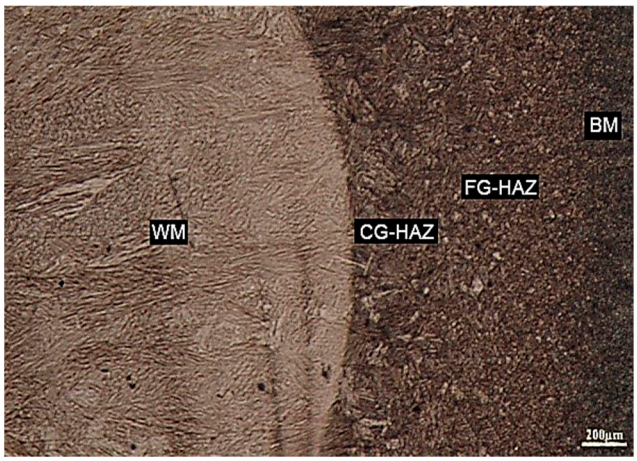

Figure 3. Optical image of weld region in sample No. 5 with a heat input of 2.229 kJ/mm showing WM, HAZ, and base metal.

According to Figure 5 showing the microstructure of HAZ, two distinct regions of fine grain HAZ (FG-HAZ) and coarse grain HAZ (CG-HAZ) can be observed. CG-HAZ was adjacent to the weld zone and by further moving away from the FZ, FG-HAZ was observed. It is well-known that microstructural changes in GTAW are dependent on welding thermal cycle and hardenability [28]. In CG-HAZ temperature peak during welding reached single-phase austenite which during cooling most likely transformed into martensite. Due to the dissolution of carbides grains increased in size compared to the base metal. The amount of grain growth was directly related to heat input; with higher heat input the size of grains further increased. The temperature only reached the ferrite–austenite region in FG-HAZ thus there was a chance for austenite nucleation. It can be concluded that during the cooling process part of the austenite grains transformed into pearlite and the rest turned into martensite. As a result, the final microstructure of FG-HAZ was most likely composed of ferrite-pearlite and martensite phases. The difference in FZ and CG-HAZ microstructure was because carbides, nitrides, and carbonitrides were dissolved in weld metal during welding creating larger initial austenite grains compared to CG-HAZ. However, in HAZ smaller grain austenite was present leading to finer martensitic microstructure.

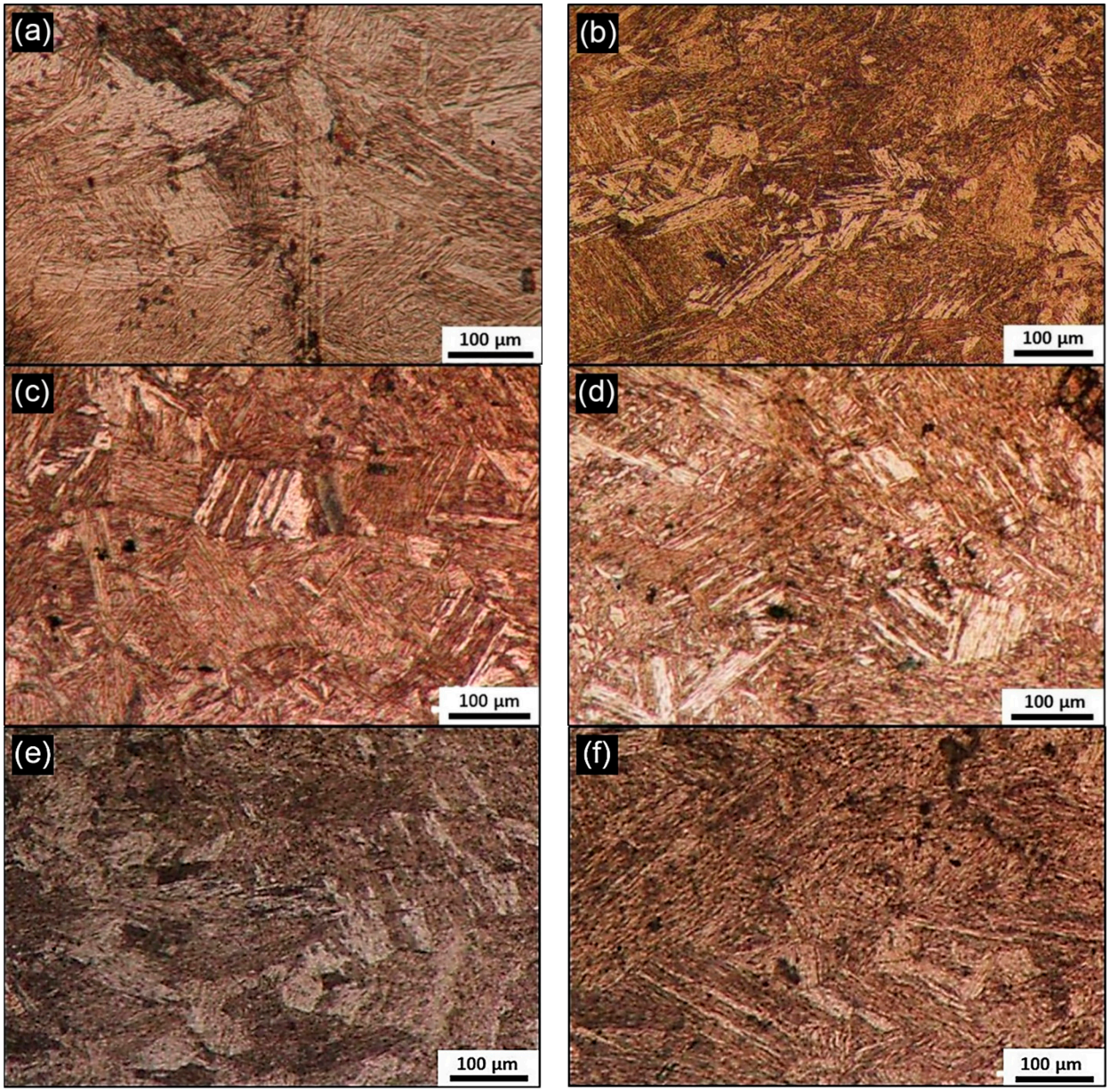

Figure 4. Effect of heat input on fusion zone microstructure, (**a**) 1.764 kJ/mm, (**b**) 1.995 kJ/mm, (**c**) 2.035 kJ/mm, (**d**) 2.132 kJ/mm, (**e**) 2.229 kJ/mm, (**f**) 2.33 kJ/mm.

3.2. Mechanical Properties of Joints

Figure 6 shows the failed samples after tensile testing. As can be seen, failure occurred in the base metal, in all samples. Due to the presence of martensitic microstructure in the fusion zone and HAZ weld region is stronger than the rest of the weldment while lower strength is expected in base metal owing to ferrite/pearlite microstructure which led to failure in that zone. The mechanical properties of joints in high-quality welds should be equal to or higher than the base metal [29,30]. Thus, S5500MC steel was successfully welded using the GTAW process even for the highest heat input in which it would be expected to see the lowest strength in the weld region and largest width for the weld zone and the HAZ.

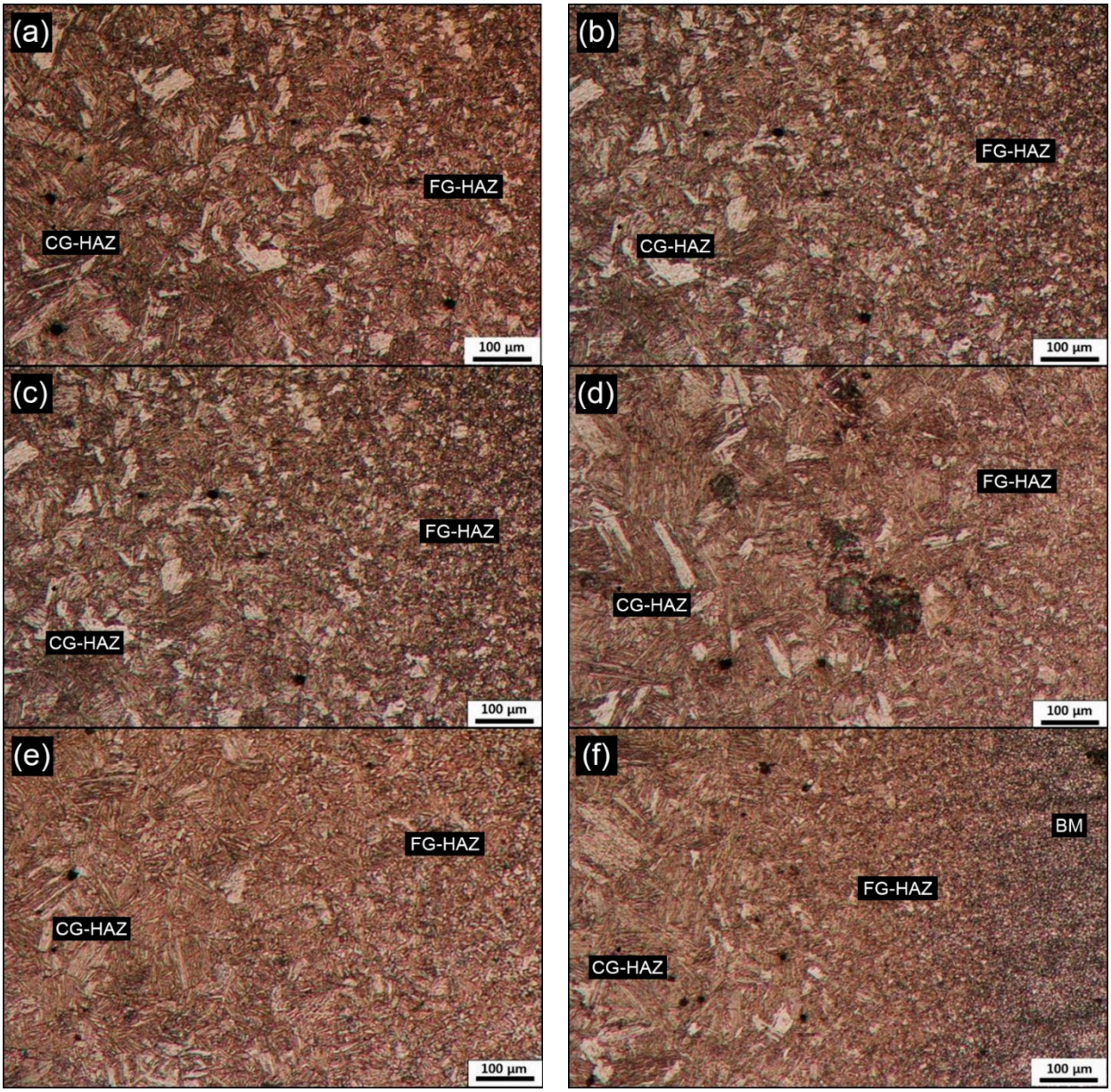

Figure 5. Effect of heat input on microstructure of HAZ, (**a**) 1.764 kJ/mm, (**b**) 1.995 kJ/mm, (**c**) 2.035 kJ/mm, (**d**) 2.132 kJ/mm, (**e**) 2.229 kJ/mm, (**f**) 2.33 kJ/mm.

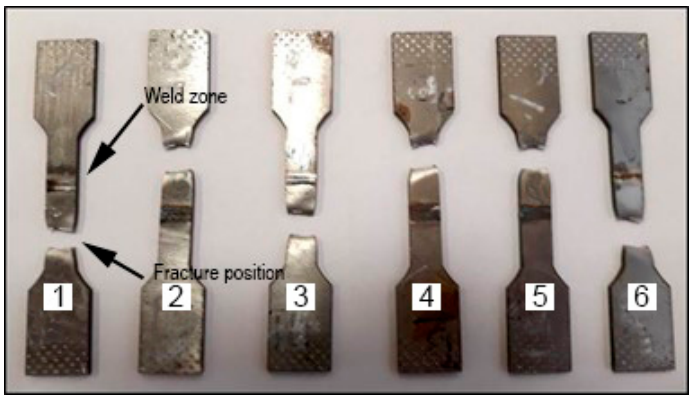

Figure 6. Tensile samples with heat inputs ranging from 1.764 kJ/mm (sample No.1) to 2.33 kJ/mm (sample No.6) after fracture, showing failure in base metal.

The tensile properties of welded joints are given in Table 4. The maximum tensile strength of around 680 MPa and yield strength of 580 MPa were observed in all samples indicating base metal failure in all samples and higher strength of weld metal. The stress–strain curve and SEM image of the fractured surface of the sample with a heat input of 2.33 kJ/mm (sample No.6) are presented in Figure 7a,b, respectively. The stress–strain curve shows a maximum yield strength of around 589 MPa and tensile strength of 675 MPa which are similar to that of base metal. Dimples can be seen in the SEM image indicating typical ductile fracture which is expected owing to ductile ferrite matrix of S500MC base metal, the region of failure. It is well-known that carbides present in grain boundary play a significant role in the fracture of HSLA steels as they can nucleate microcracks [31]. Most likely carbides present in the S500MC base metal matrix, like other HSLA steels, acted as crack initiation sites resulting in the micro void formation and final failure.

Table 4. Tensile properties of welded joints.

Experiment No.	Tensile Strength (MPa)	Yield Strength (MPa)
1	690	580
2	685	550
3	680	562
4	676	590
5	684	575
6	675	589

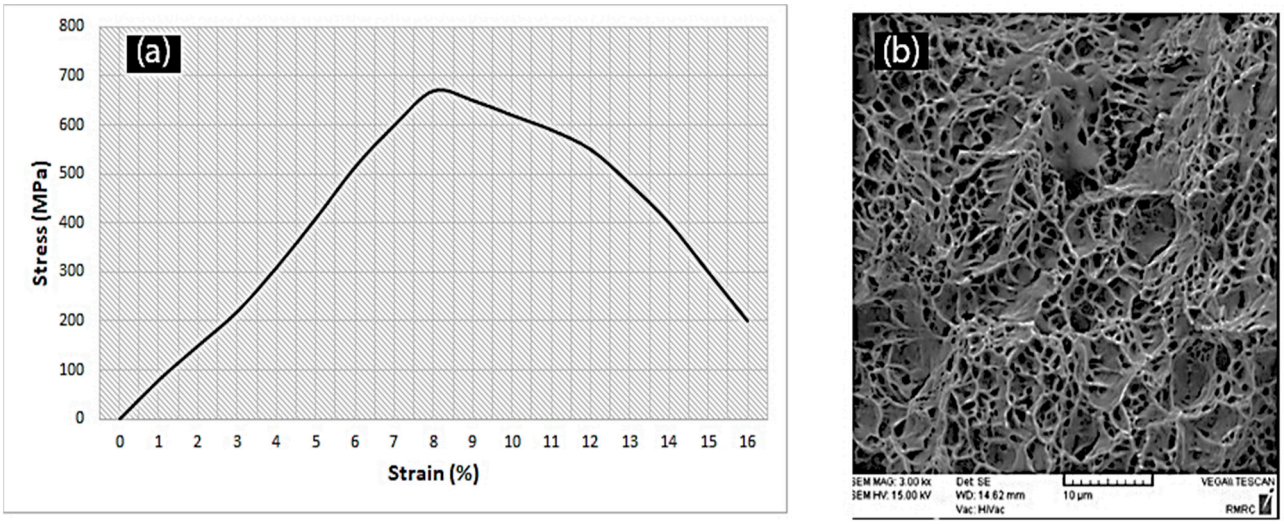

Figure 7. (**a**) Stress–strain curve of welded joint with a heat input of 2.33 kJ/mm, (**b**) SEM image of the fracture surface of 2.33 kJ/mm sample indicating ductile fracture.

4. Conclusions

In this paper, the effect of different levels of heat input on microstructure and tensile property during the gas tungsten arc welding of S500MC HSLA was investigated. These conclusions can be drawn from the observations:

1. The microstructure of base metal consisted of ferrite and pearlite in the normalized state. However, the weld metal microstructure altered to most likely lath martensite and retained austenite. By increasing the heat input the size of martensitic packs was increased due to the dissolution of carbides. The amount of retained austenite also increased by the increase in heat input.
2. Heat-affected zone microstructure could be divided into two regions, namely, coarse grain HAZ (CG-HAZ) near the weld zone and fine grain HAZ (FG-HAZ) adjacent to the base metal. In CG-HAZ, a fine martensitic microstructure was observed while in FG-HAZ, a combination of pearlite and martensite formed as the final microstructure.

3. Although microstructural changes occurred in FZ and HAZ, this did not negatively affect the tensile strength, and maximum tensile strength of 690 MPa was achieved. The presence of martensite microstructure in weld metal apparently increased the strength in that region leading to failure in the base metal.

Author Contributions: Conceptualization, K.K. and M.M.; Data curation, K.K.; Formal analysis, K.K., F.N., H.M., A.S., M.M., D.G.W. and M.B.; Funding acquisition, M.M.; Investigation, K.K., F.N., H.M., A.S., M.M., D.G.W. and M.B.; Methodology, K.K., F.N., H.M. and M.M.; Project administration, M.M.; Supervision, F.N., H.M. and M.M.; Visualization, K.K.; Writing—original draft, K.K. and A.S.; Writing—review & editing, K.K., F.N., H.M., A.S., M.M., D.G.W. and M.B. All authors have read and agreed to the published version of the manuscript.

Funding: This research received no external funding.

Data Availability Statement: All data genertated in this study can be found within the paper.

Conflicts of Interest: The authors declare no conflict of interest.

References

1. Karganroudi, S.S.; Moradi, M.; Attar, M.A.; Rasouli, S.A.; Ghoreishi, M.; Lawrence, J.; Ibrahim, H. Experimental and Numerical Analysis on TIG Arc Welding of Stainless Steel Using RSM Approach. *Metals* **2021**, *11*, 1659. [CrossRef]
2. Sathish, T.; Kumar, S.D.; Muthukumar, K.; Karthick, S. Natural inspiration technique for the parameter optimization of A-GTAW welding of naval steel. *Mater. Today Proc.* **2020**, *21*, 843–846. [CrossRef]
3. Thakur, P.P.; Chapgaon, A.N. A review on effects of GTAW process parameters on weld. *IJRASET* **2016**, *4*, 136–140.
4. Pujari, K.; Patil, D.; Mewundi, G. Selection of GTAW process parameter and optimizing the weld pool geometry for AA 7075-T6 Aluminium alloy. *Mater. Today Proc.* **2018**, *5*, 25045–25055. [CrossRef]
5. Cabibbo, M.; Fabrizi, A.; Merlin, M.; Garagnani, G.L. Effect of thermo-mechanical treatments on the microstructure of micro-alloyed low-carbon steels. *J. Mater. Sci.* **2008**, *43*, 6857–6865. [CrossRef]
6. Saadati, M.; Nobarzad, A.K.E.; Jahazi, M. On the hot cracking of HSLA steel welds: Role of epitaxial growth and HAZ grain size. *J. Manuf. Process.* **2019**, *41*, 242–251. [CrossRef]
7. Jindal, S.; Chhibber, R.; Mehta, N. Issues in Welding of HSLA Steels. *Adv. Mater. Res.* **2011**, *365*, 44–49. [CrossRef]
8. Frih, I.; Montay, G.; Adragna, P.-A. Microstructure, Hardness, and Residual Stress Distributions in T-Joint Weld of HSLA S500MC Steel. *Met. Mater. Trans. A* **2017**, *48*, 1103–1110. [CrossRef]
9. Karademir, I.; Celik, M.B.; Husem, F.; Maleki, E.; Amanov, A.; Unal, O. Effects of constrained groove pressing, severe shot peening and ultrasonic nanocrystal surface modification on microstructure and mechanical behavior of S500MC high strength low alloy automotive steel. *Appl. Surf. Sci.* **2021**, *538*, 147935. [CrossRef]
10. Coelho, R.; Corpas, M.; Moreto, J.; Jahn, A.; Standfuß, J.; Kaysser-Pyzalla, A.; Pinto, H. Induction-assisted laser beam welding of a thermomechanically rolled HSLA S500MC steel: A microstructure and residual stress assessment. *Mater. Sci. Eng. A* **2013**, *578*, 125–133. [CrossRef]
11. Fydrych, D.; Łabanowski, J.; Rogalski, G.; Haras, J.; Tomków, J.; Świerczyńska, A.; Jakóbczak, P.; Kostro, Ł. Weldability of S500MC Steel in Underwater Conditions. *Adv. Mater. Sci.* **2014**, *14*, 37–45. [CrossRef]
12. Alipooramirabad, H.; Ghomashchi, R.; Paradowska, A.; Reid, M. Residual stress- microstructure- mechanical property interrelationships in multipass HSLA steel welds. *J. Mater. Process. Technol.* **2016**, *231*, 456–467. [CrossRef]
13. Cao, X.; Wanjara, P.; Huang, J.; Munro, C.; Nolting, A. Hybrid fiber laser—Arc welding of thick section high strength low alloy steel. *Mater. Des.* **2011**, *32*, 3399–3413. [CrossRef]
14. Dong, H.; Hao, X.; Deng, D. Effect of Welding Heat Input on Microstructure and Mechanical Properties of HSLA Steel Joint. *Met. Microstruct. Anal.* **2014**, *3*, 138–146. [CrossRef]
15. Moon, J.; Kim, S.-J.; Lee, C. Effect of thermo-mechanical cycling on the microstructure and strength of lath martensite in the weld CGHAZ of HSLA steel. *Mater. Sci. Eng. A* **2011**, *528*, 7658–7662. [CrossRef]
16. Musa, M.H.A.; A Maleque, M.; Ali, M.Y. An Investigation of TIG welding parameters on microhardness and microstructure of heat affected zone of HSLA steel. *IOP Conf. Ser. Mater. Sci. Eng.* **2018**, *290*, 12041. [CrossRef]
17. Oyyaravelu, R.; Kuppan, P.; Arivazhagan, N. Metallurgical and mechanical properties of laser welded high strength low alloy steel. *J. Adv. Res.* **2016**, *7*, 463–472. [CrossRef]
18. Miletić, I.; Ilić, A.; Nikolić, R.R.; Ulewicz, R.; Ivanović, L.; Sczygiol, N. Analysis of Selected Properties of Welded Joints of the HSLA Steels. *Materials* **2020**, *13*, 1301. [CrossRef]
19. Skariya, P.D.; Satheesh, M.; Dhas, J.E.R. Optimizing parameters of TIG welding process using grey wolf optimization concerning 15CDV6 steel. *Evol. Intell.* **2018**, *11*, 89–100. [CrossRef]
20. Pamnani, R.; Vasudevan, M.; Vasantharaja, P.; Jayakumar, T. Optimization of A-GTAW welding parameters for naval steel (DMR 249 A) by design of experiments approach. *Proc. Inst. Mech. Eng. Part L J. Mater. Des. Appl.* **2017**, *231*, 320–331. [CrossRef]

21. Sallaba, F.; Rolof, F.; Ehlers, S.; Walters, C.L.; Braun, M. Relation between the Fatigue and Fracture Ductile-Brittle Transition in S500 Welded Steel Joints. *Metals* **2022**, *12*, 385. [CrossRef]
22. Talaş, Ş. The assessment of carbon equivalent formulas in predicting the properties of steel weld metals. *Mater. Des.* **2010**, *31*, 2649–2653. [CrossRef]
23. Niles, R.W.; Jackson, C.E. Weld thermal efficiency of the GTAW process. *Weld. J.* **1975**, *54*, 25.
24. Tomków, J.; Świerczyńska, A.; Landowski, M.; Wolski, A.; Rogalski, G. Bead-on-Plate Underwater Wet Welding on S700MC Steel. *Adv. Sci. Technol. Res. J.* **2021**, *15*, 288–296. [CrossRef]
25. CChen, L.; Nie, P.; Qu, Z.; Ojo, O.; Xia, L.; Li, Z.; Huang, J. Influence of heat input on the changes in the microstructure and fracture behavior of laser welded 800MPa grade high-strength low-alloy steel. *J. Manuf. Process.* **2020**, *50*, 132–141. [CrossRef]
26. Yang, X.; Di, X.; Liu, X.; Wang, D.; Li, C. Effects of heat input on microstructure and fracture toughness of simulated coarse-grained heat affected zone for HSLA steels. *Mater. Charact.* **2019**, *155*, 109818. [CrossRef]
27. Kou, S. *Welding Metallurgy*; John Wiley & Sons, Inc.: Hoboken, NJ, USA, 2003.
28. Fei, Z.; Pan, Z.; Cuiuri, D.; Li, H.; Wu, B.; Ding, D.; Su, L. Effect of Heat Input on Weld Formation and Tensile Properties in Keyhole Mode TIG Welding Process. *Metals* **2019**, *9*, 1327. [CrossRef]
29. Pereira, A.B.; de Melo, F.J.M.Q. Quality assessment and process management of welded joints in metal construction—A review. *Metals* **2020**, *10*, 115. [CrossRef]
30. Moradi, M.; Khorram, A.; Fallah, M.M. Nd:YAG Laser Welding of Ti 6-Al-4V: Mechanical and Metallurgical Properties. *Lasers Eng.* **2019**, *43*, 21–33.
31. Ghosh, A.; Ray, A.; Chakrabarti, D.; Davis, C. Cleavage initiation in steel: Competition between large grains and large particles. *Mater. Sci. Eng. A* **2013**, *561*, 126–135. [CrossRef]